SE9700089
ISSN 1102-2051
ISRN KTH/ALF/R--96/5--SE

KTH

Thomson scattering in the EXTRAP-T2 reversed-field pinch

A. Welander

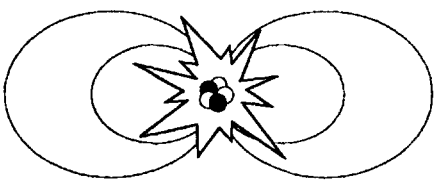

Research and Training programme on
CONTROLLED THERMONUCLEAR FUSION
AND PLASMA PHYSICS
(Association EURATOM/NFR)

FUSION PLASMA PHYSICS
ALFVÉN LABORATORY
ROYAL INSTITUTE OF TECHNOLOGY
S-100 44 STOCKHOLM SWEDEN

TRITA-ALF-1996-05
ISRN KTH/ALF/R--96/5--SE

Thomson scattering in the EXTRAP-T2 reversed-field pinch

A. Welander

Stockholm, November 1996

The Alfvén Laboratory
Division of Fusion Plasma Physics
Royal Institute of Technology
S-100 44 Stockholm, Sweden
(Association EURATOM/NFR)

Printed by
the Alfvén Laboratory
Fusion Plasma Physics Division
Royal Institute of Technology
S-100 44 Stockholm

Thomson scattering in the EXTRAP-T2 reversed-field pinch

A. Welander

Abstract

A Thomson scattering system has been installed on the EXTRAP-T2 reversed-field pinch (RFP) experiment. The system measures the electron density and temperature in three radial points using three spectral channels. A description of the system, the calibration techniques and examples of data obtained are given. The error bars for the electron temperature measurements are estimated to be $\leq 10\%$ for typical T2-plasmas.

Introduction

The EXTRAP-T2 RFP shown in Fig. 1 is a medium sized experiment (R/a = 1.24 m/ 0.183 m), and is the former OHTE experiment [1]. The main parameters of the experiment are given in Table 1. The vessel has a resistive shell, with a magnetic penetration time, $\tau = 1.5$ ms and the plasma first wall is completely covered by graphite. The Thomson scattering system described here measures the electron density and temperature profiles in the central region of the plasma at one single time into the discharge. As a complement, the edge region is diagnosed by electrostatic probes. information about the time evolution of the line-of-sight integrated density is given by a one chord CO_2 laser interferometer and time dependent information about the temperature is given by the soft x-ray ratio technique.

The Thomson scattering system

A schematic view of the Thomson scattering system [2] is shown in Fig. 2. It can be divided into three systems, the ruby laser beam and optics, the viewing optics, and the data acquisition system.

Ruby laser beam and optics

A Quantel ruby laser is used to fire a horizontally polarised 10 J laser pulse with a duration of 50 ns and with a wavelength of 694.3 nm. The beam is expanded by lenses L1 and L2 to reduce the power density and then guided by mirrors M1, M2 and M3 to lens L3 where it is focused down to a diameter of roughly 1 mm in the center of the plasma. On exit from the machine, the laser energy is absorbed in a green glass laser dump which is oriented at the Brewster angle to avoid reflections. When the beam passes

through the entrance window to the machine, some of the light will inevitably be scattered, mostly at low angles. Some of this light and light from other sources will, after multiple reflections, reach the viewing optics and disturb the measurement. A series of apertures after the window are used to minimise such light termed stray light.

Viewing optics

Scattered light from three points along the laser beam at minor radii r = [0, 52, 103] mm (r/a = [0, 0.28, 0.56]) is imaged onto three different fibers. The fibers are of varying lengths to allow time multiplexing of the light from the different points. The light is guided to a three-spectral-channel spectrometer. The dispersion of light in the spectrometer is provided by interference filters and light detection is provided by three avalanche photo detectors (APD) which are covered by the interference filters. Inside the spectrometer, the guided light from the three fibers is imaged onto interference filter number 1 where a selected wavelength range of light is transmitted and detected by APD1. The image on the first interference filter is then imaged onto the second interference filter where a selected range of the remaining light is transmitted to APD2. Finally a selected range of light is transmitted through the third interference filter and detected by APD3.

Data acquisition

The detector signals are stored using a 2 GHz digital 4 channel oscilloscope. In order to trigger the oscilloscope and measure the laser power, there is a fiber leading to a simple photo diode mounted behind M3. This detector receives a part of the small fraction of light which is transmitted rather than reflected by M3. A diffuser in front of the photo diode fiber ensures that the light entering the fiber is representative of the cross section integrated power of the beam. The photo diode signal is recorded along with the signals from the spectrometer on the fast digitising oscilloscope and transferred to a computer for evaluation of the electron density and temperature data points.

Calibration

The time integrated signals from the spectrometer can be written as:

$$S_{ij}^{tot} = \iint_{\lambda,t} G_{ij}(\lambda) \times (I_{TS}(n_e, T_e) + I_{stray}) d\lambda dt \text{ (pVs)}, \tag{1}$$

where index i denotes a spectral channel and index j denotes a spatial point in the plasma, λ is wavelength, t is time, $G_{ij}(\lambda)$ are the instrumental functions and the Thomson spectrum I_{TS} is given by [3]:

$$I_{TS} = n_e L P_0 \frac{r_e^2}{\lambda_0} C(\alpha) A^{-1}(\varepsilon, \theta) \exp\left[-2\alpha B(\varepsilon, \theta)\right] \text{ (W sr}^{-1}\text{ nm}^{-1}), \tag{2}$$

where,

$$A(\varepsilon, \theta) = (1+\varepsilon)^3 \sqrt{2(1-\cos\theta)(1+\varepsilon) + \varepsilon^2} \tag{3a}$$

$$B(\varepsilon, \theta) = \sqrt{1 + \frac{\varepsilon^2}{2(1-\cos\theta)(1+\varepsilon)}} - 1 \tag{3b}$$

$$C(\alpha) = \sqrt{\frac{\alpha}{\pi}} \left(1 - \frac{15}{16}\alpha^{-1} + \frac{345}{512}\alpha^{-2} + \ldots\right) \tag{3c}$$

and

$$\varepsilon = \frac{\lambda}{\lambda_0} - 1$$

$$\alpha = \frac{m_e c^2}{2kT_e}$$

$$r_e \equiv \frac{e^2}{4\pi\varepsilon_0 m_e c^2} .$$

Here θ is the angle between the incident laser beam and the scattered light, r_e is the classical electron radius, λ_0 = 694.3 nm is the ruby laser wavelength, L is the length of beam being observed and P_0 is the laser power.

In order to deduce density and temperature it is necessary to know the instrumental functions $G_{ij}(\lambda)$ and the stray light contributions:

$$S_{ij}^{stray} = \iint_{\lambda,t} G_{ij}(\lambda) \times I_{stray} d\lambda dt.$$

The stray light terms S_{ij}^{stray} are easily measured by firing the laser with no plasma present in the machine. The instrumental functions $G_{ij}(\lambda)$ were determined in three steps.

Shapes of instrumental functions

In the first step the shapes of the instrumental functions were measured using the set-up shown in Fig. 3. A fiber of the same kind as the ones that are used in the Thomson scattering system was connected to the spectrometer and illuminated by the output from a monochromator. The wavelength scale of the monochromator was scanned through the region of interest and the three signals from the spectrometer were read into a computer. This was then compared to the output from a calibrated detector. The shapes depend mainly on the transmissions of the filters in the spectrometer, but also on lens and fiber transmissions and the response of the APDs. When the spectrometer is operated in the Thomson scattering mode, the APD amplifiers are AC-coupled to filter out the plasma light background level. In this calibration the pulses are much longer and the amplifiers are therefore DC-coupled in this case.

Relative amplitudes

The second step was to determine the relative amplitudes of instrumental functions for the fibers used on the experiment, i.e. the ratios $G_{1j} / G_{2j} / G_{3j}$. This calibration was necessary since the first calibration was made with a test fiber. The main difference in the instrumental functions when the correct fibers are used is a change of the amplitudes of the instrumental functions and not their shapes. Also, the frequency dependence of the amplifiers is accounted for in this step, which is necessary since the amplifiers were DC-coupled in the first calibration and have different amplifications when they are AC-coupled. In order to determine the ratios a light emitting diode (LED) was used. The spectrum from the LED which is very similar to a Thomson scattering spectrum was first measured (Fig. 4). The unit that holds the viewing optics and fibers can be moved up from its nominal position on the window to the T2 vessel and down again in a reproducible manner, thus allowing for an in situ calibration using the LED source. The unit was moved up and the LED was placed underneath. The LED can be pulsed on the same time scale as the ruby laser and the intensity of the emitted light is equal to that of Thomson scattered light. Consequently the LED is a suitable light source for simulating Thomson scattered light. The signals from the spectrometer were recorded on the oscilloscope and averaged over several thousand pulses to get good statistical accuracy.

Absolute calibration

Finally, the absolute values of the instrumental functions for spectral channel number 3 can be measured using Raman scattering from nitrogen. The functions $G_{ij}(\lambda)$ are then fully determined.

Raman scattered light comes in discrete lines, their intensities given by [4]:

$$I_{J\to J'} = n_{N_2} L P_0 F_J \sigma_{J\to J'} \quad (\mathrm{W\ sr^{-1}}). \tag{4}$$

Here J is the rotational-angular-momentum quantum number, P_0 is the ruby laser power, n_{N_2} is the number density of nitrogen molecules and L is the length of the laser beam being viewed. Allowed transitions are to $J' = J \pm 2$. The associated line is shifted from the ruby laser wavelength by $\Delta\lambda = 0.0959(4J+6)$ (nm) when $J' = J+2$ and by $\Delta\lambda = -0.0959(4J-2)$ (nm) when $J' = J-2$. F_J is the fraction of molecules in the state J. For nitrogen at a room temperature of 295 K, F_J is given to a good approximation by:

$$F_J = \frac{g_J(2J+1)}{463.7}\exp\left(-\frac{J(J+1)}{103}\right). \tag{5}$$

where g_J is a statistical weight factor, dependent on nuclear spin. Its value for nitrogen is:

$$g_J = \begin{cases} 6, & even\ J \\ 3, & odd\ J \end{cases}.$$

Finally $\sigma_{J\to J'}$ is the differential cross section, a valid expression in this case (with λ in nm) is:

$$\sigma_{J\to J+2} = 9.52\times10^{-23}\frac{(J+1)(J+2)}{(2J+1)(2J+3)}(\lambda_0 + \Delta\lambda_{J\to J'})^{-4}\ (\mathrm{m^2\ sr^{-1}}) \tag{6a}$$

and

$$\sigma_{J\to J-2} = 9.52\times10^{-23}\frac{J(J-1)}{(2J+1)(2J-1)}(\lambda_0 + \Delta\lambda_{J\to J'})^{-4}\ (\mathrm{m^2\ sr^{-1}}). \tag{6b}$$

The Raman spectrum for nitrogen at room temperature is shown in Fig. 5 together with the instrumental function for spectral channel number 3. The signals obtained at different nitrogen pressures are shown in Fig. 6. On spectral channels 1 and 2, the

increase of the signal with nitrogen pressure is caused by Rayleigh scattering which occurs at the ruby laser wavelength. The increase of the signals on channel 3 with nitrogen pressure is also caused by Rayleigh scattering to some extent. This part can be subtracted since the ratios of Rayleigh scattered light to stray light is the same on every spectral channel and these ratios are given by the signals on channel 2. The instrumental functions are shown in Fig. 7.

Data evaluation and error analysis

An example of raw data is shown in Fig. 8. The best estimate of the pulse values is achieved by using the known information on the pulse shapes from the photo diode signal. The light pulses in the 20, 50 and 80 m fibers arrive later than the pulse in the photo diode fiber by 31, 177 and 323 ns respectively. The stray light pulses are delayed an extra 6.5, 7.5 and 10 ns because the stray light is reflected a number of times inside the T2 vessel before reaching the viewing optics. The background plasma light is sufficiently slowly varying on the time scale of the ruby laser pulse to be adequately described with a polynomial function of time. The most probable signals are thus found from a least-square fit of a polynomial and the three pulse shapes to the measured data. The standard deviation of the pulse value will then be:

$$\Delta S_{ij} = \Delta t_{sample} b \frac{\sum D_k}{\sqrt{\sum D_k^2}} \text{ (pVs)} \qquad (7)$$

here Δt_{sample} is the sampling time ($\Delta t_{sample} = 0.5$ ns), b is the standard deviation of the noise, D_k is sample number k of the photo diode signal. The error bar for 90 % confidence is $1.64\Delta S_{ij}$. The error bars obtained when the LED described above was used to deliver 100 identical pulses, are in very good agreement with the theoretical prediction.

The next step is to calculate the most probable n_e and T_e values from the obtained pulse values. The expression for the probability that fiber j sees a density, n_e and temperature, T_e is:

$$p_j(n_e, T_e) = N \exp\left[-\sum_i \frac{\left(S_{ij} - n_e T_{ij}(T_e)\right)^2}{2\left(\Delta S_{ij}\right)^2} \right], \tag{8}$$

where S_{ij} is the measured pulse value on channel i from fiber j and $n_e T_{ij}(T_e)$ is the calculated pulse value for n_e, T_e. The probability distribution for T_e can be found analytically as:

$$p_j(T_e) = N \sqrt{\frac{\pi}{2}} \exp\left[\frac{\eta^2}{\gamma} - \chi \right] / \sqrt{\gamma} \tag{9}$$

$$\gamma = \sum_i \frac{T_{ij}^2}{2\left(\Delta S_{ij}\right)^2} \tag{10a}$$

$$\eta = \sum_i \frac{S_{ij} T_{ij}}{2\left(\Delta S_{ij}\right)^2} \tag{10b}$$

$$\chi = \sum_i \frac{S_{ij}^2}{2\left(\Delta S_{ij}\right)^2} \tag{10c}$$

whereas $p_j(n_e)$ is found numerically. Both of the distributions are very maxwellian-like in most cases with fairly low error spreads. A code has been developed to calculate the most probable value and the range for 90 % confidence for both n_e and T_e after every measurement. The average random error during the first 500 measurements (for the three different radial points r=0, 52, 103 mm) has been 3, 4, 5 % for n_e and 5, 8, 11 % for T_e, for the case when $n_e = 5 \times 10^{19}$ m^{-3}. The error is proportional to $1 / n_e$. The code will also correctly handle cases where the signal is digitally saturated and cases where the pulse is longer than the time between the pulses.

Results

Some typical temperatures measured in the EXTRAP-T2 are shown in Fig. 9. The data represents shots under different conditions. It is therefore important to note that the spread of the data is larger than the error bars. The temperature variations observed can be due to different impurity levels, power input levels or RFP parameters for example. The conclusion is that the accuracy of the Thomson scattering measurements of density and temperature is adequate so that the diagnostic can be used for studies of plasma parameters under different conditions, using a reasonable number of shots to achieve statistically relevant results.

Acknowledgements

The author is indebted to Mr. J. Tonks, Mr. B. Wilner and Mr. G. Kindberg among others for constructing many of the mechanical parts of the system and mounting them in their right places. Many thanks go also to Dr. J. Brzozowski for sharing his experience.

References

[1] P. Taylor, et al., 15:th European Conf., Dubrovnik, 1988, Europhys. Conf. Abstracts, Vol. **12B**, Part II, (1988) 573

[2] The spectrometer and light collection system was delivered by UKAEA Fusion, Culham Laboratory

[3] A. C. Selden, Culham Report CLMR-220, 1982; Phys. Lett. **79A**, 405 (1980)

[4] C. M. Penney, R. L. St. Peters, and M. Lapp, J. Opt. Soc. Amer. **64**(5), 1974 712-716

Table 1.

Extrap T2 device

Vacuum vessel & first wall

major radius (R)	1.24 m
first wall minor radius (a)	183 mm
aspect ratio (R/a)	6.8
first wall material (tiles)	graphite
tile thickness	3.2 mm
vessel material (bellows)	316 SST
bellows inside minor radius	187 mm

Resistive shell

shell minor radius	200 mm
shell thickness	0.8 mm
shell proximity (b/a)	1.09
shell material	brass
poloidal gaps	1
vertical field penetration time	1.5 ms
toroidal gaps	none
toroidal field penetration time	0.2 ms

Toroidal field

power supply total energy	1.15 MJ
helical coil minor radius	235 mm
number of poloidal turns	32

Ohmic heating

power supply total energy	2.27 MJ
iron core flux swing (with reversed bias)	5 Vs
primary coils series-parallel connected	20 turns
primary to secondary turns ratio	5:1

Vertical field

At present from OH primary currents

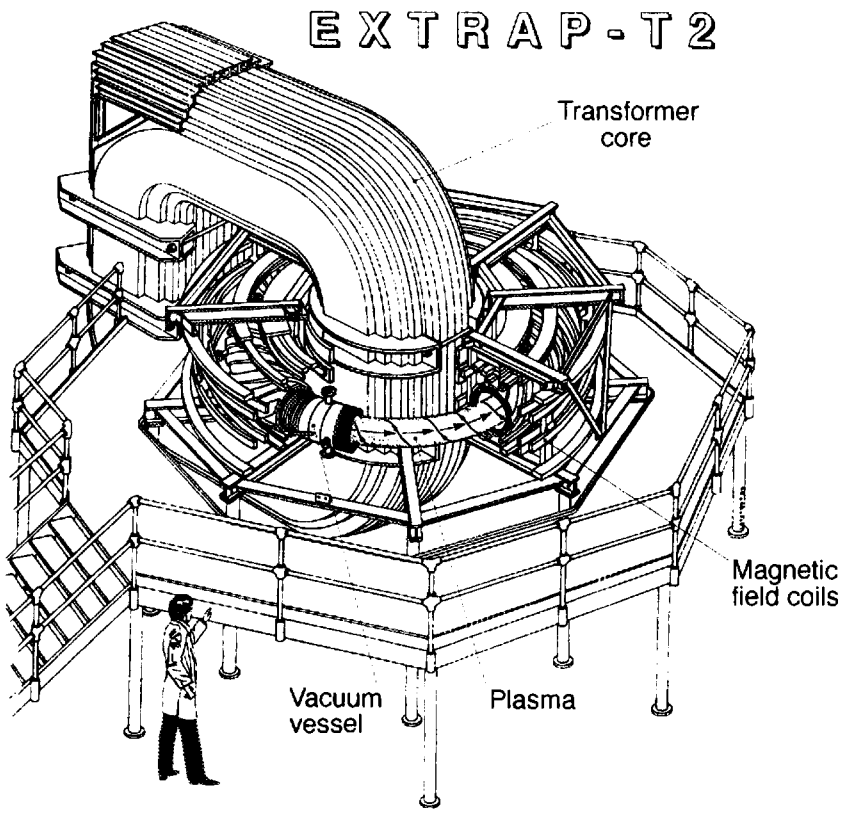

Fig. 1 The EXTRAP-T2 experiment.

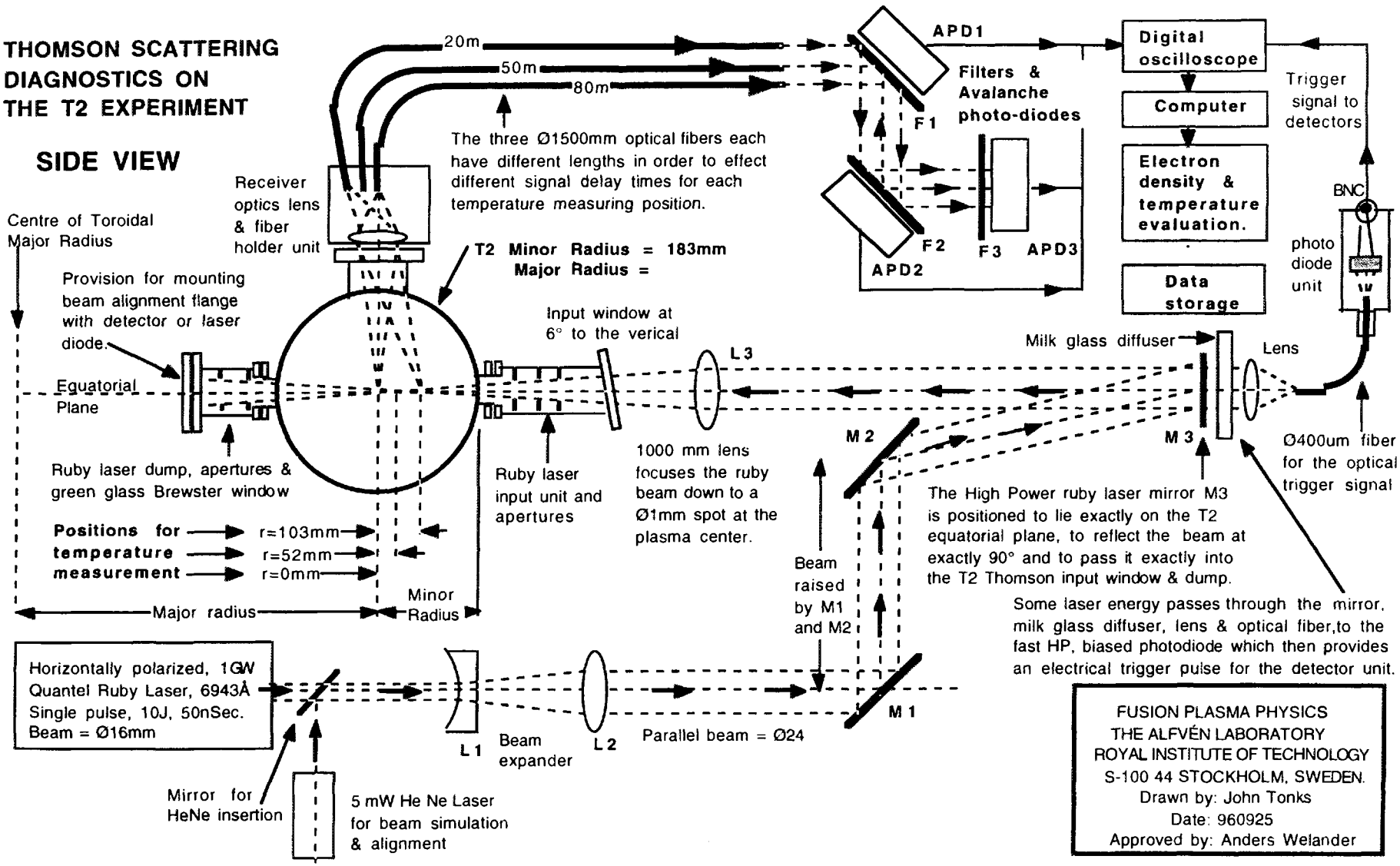

Fig. 2 A schematic view of the Thomson scattering system in use on the EXTRAP-T2 experiment.

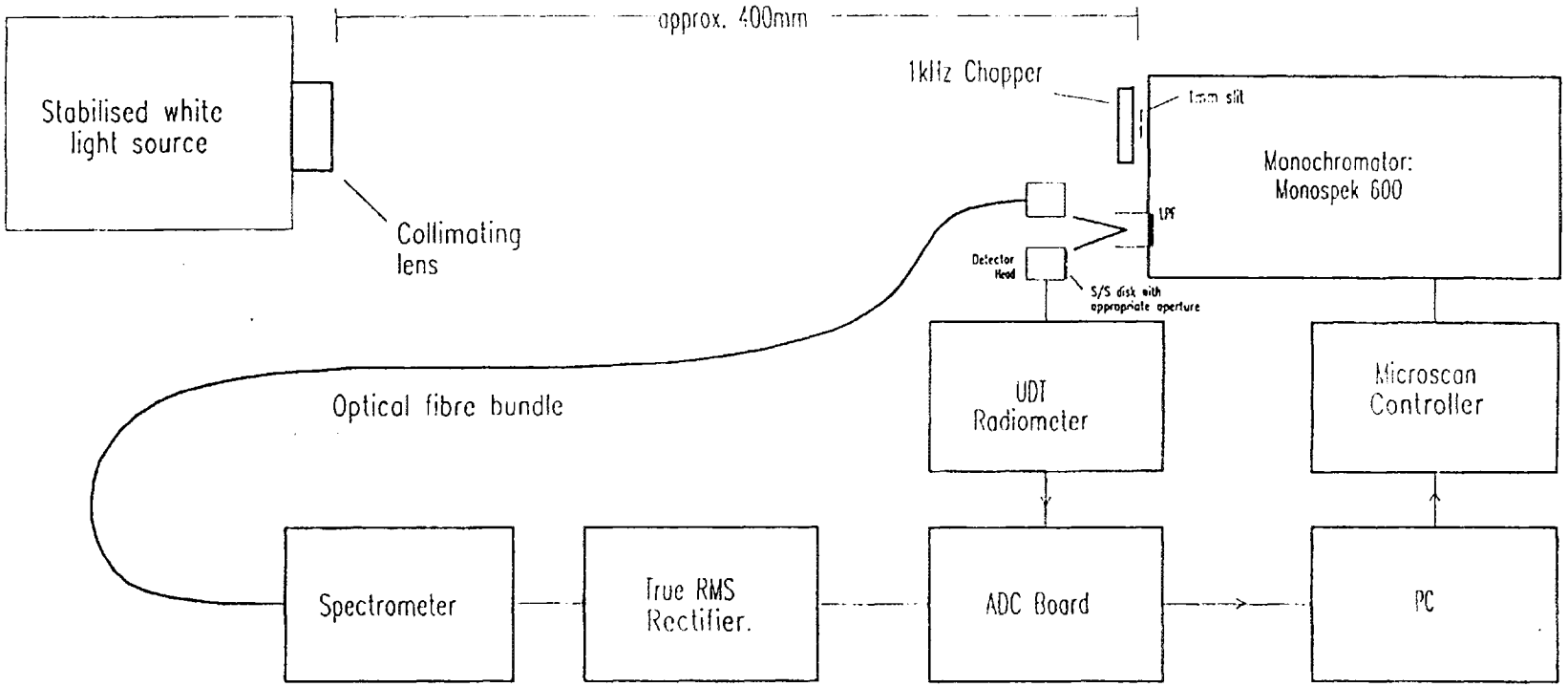

Fig. 3 The arrangement for calibration of the spectrometer.

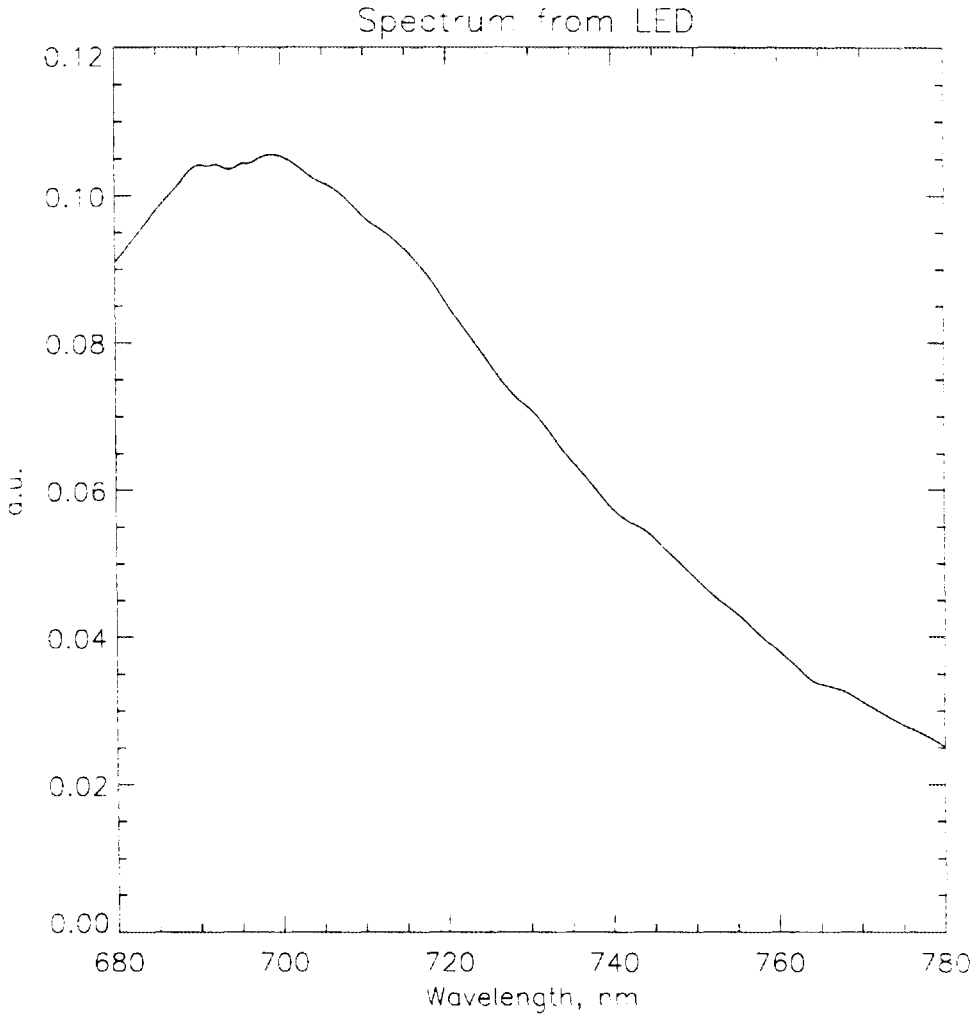

Fig. 4 The spectrum from the light emitting diode which is used in the calibration.

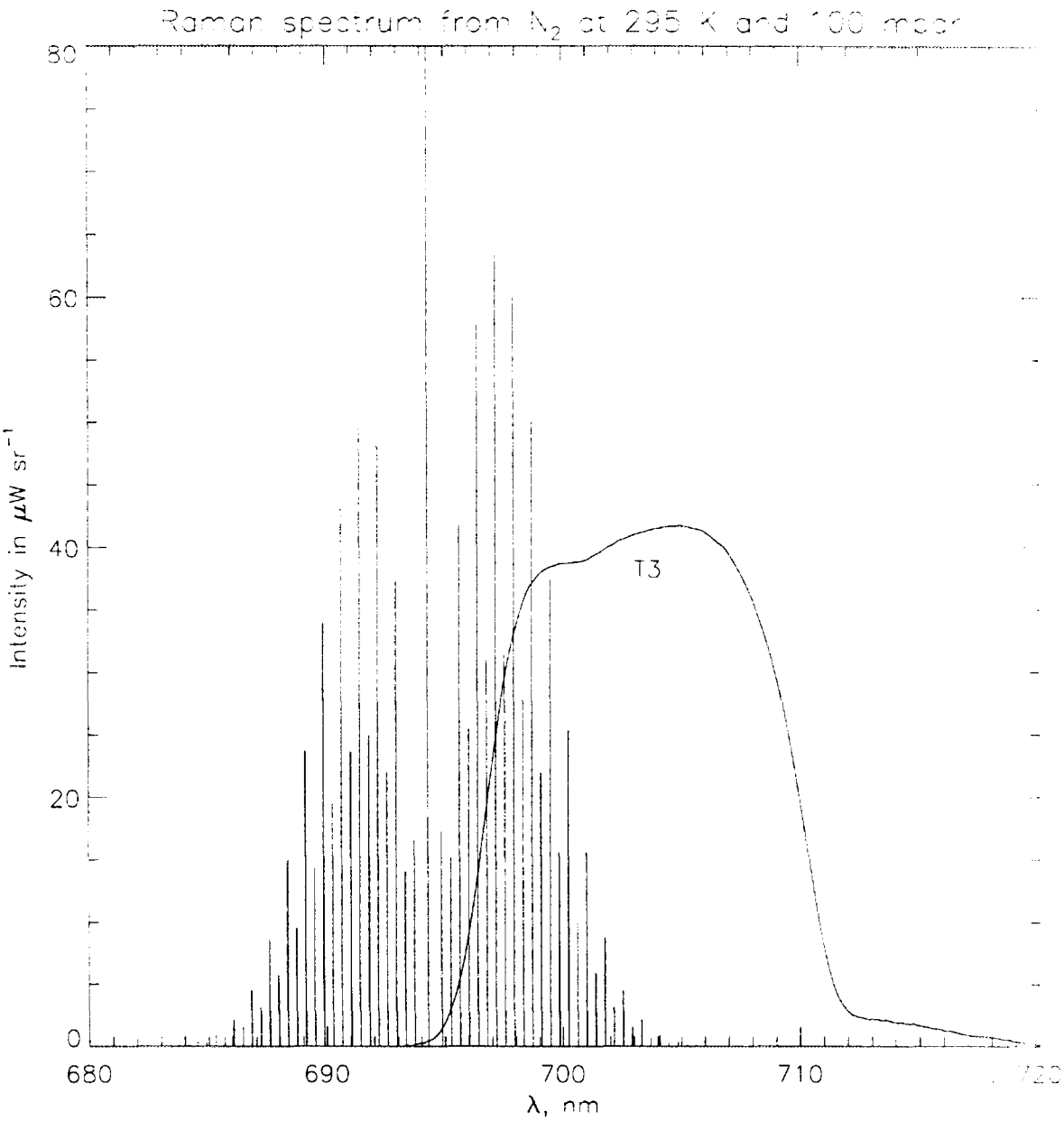

Fig. 5 The Raman spectrum from nitrogen at room temperature is shown together with the instrumental function for spectral channel number 3. The intensity at the ruby laser wavelength, 694.3 nm, is much higher than the Raman lines.

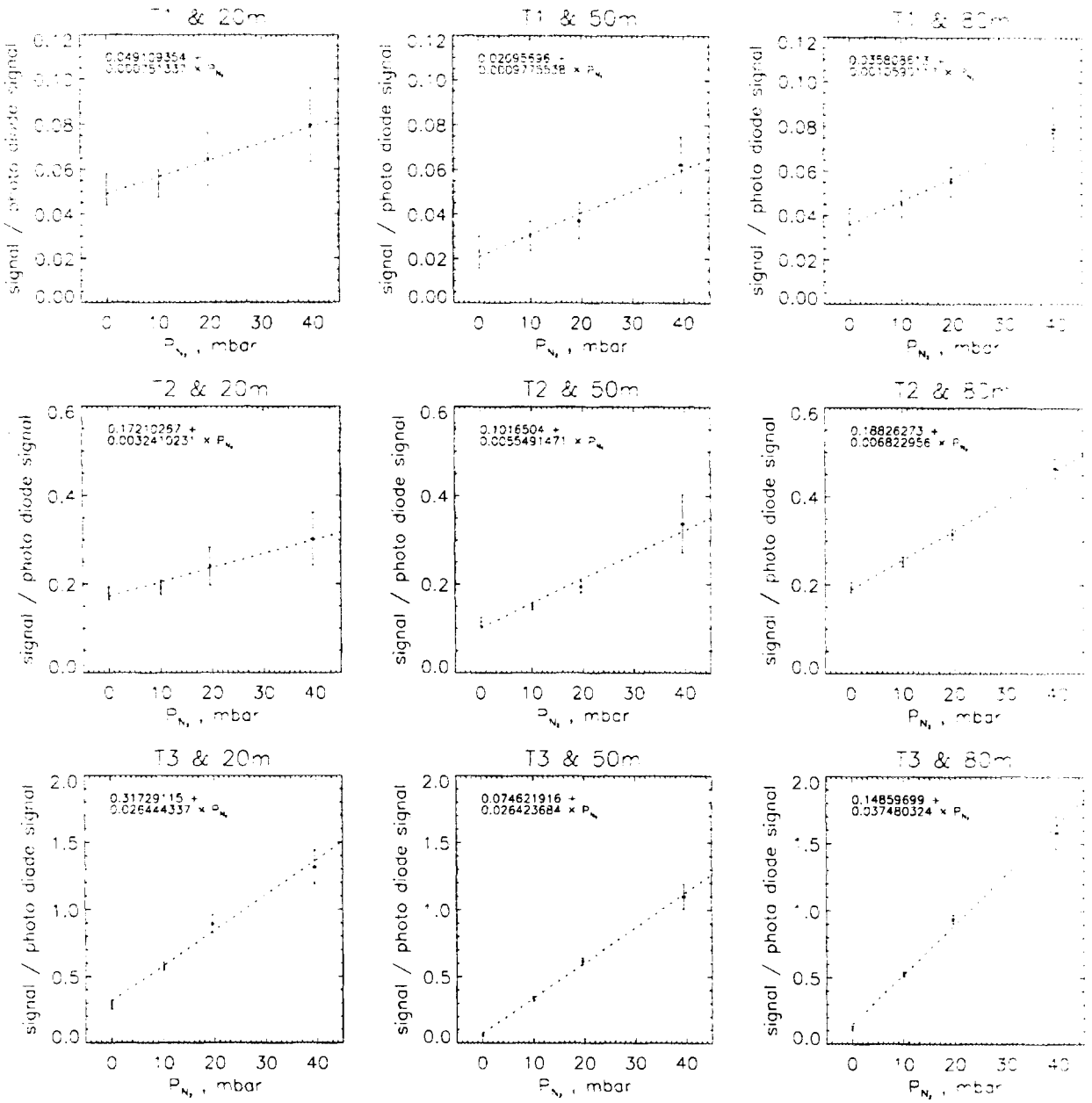

Fig. 6 The signals obtained at different nitrogen pressures.

Raman scattered light is detected by spectral channel number 3 (in the third row).

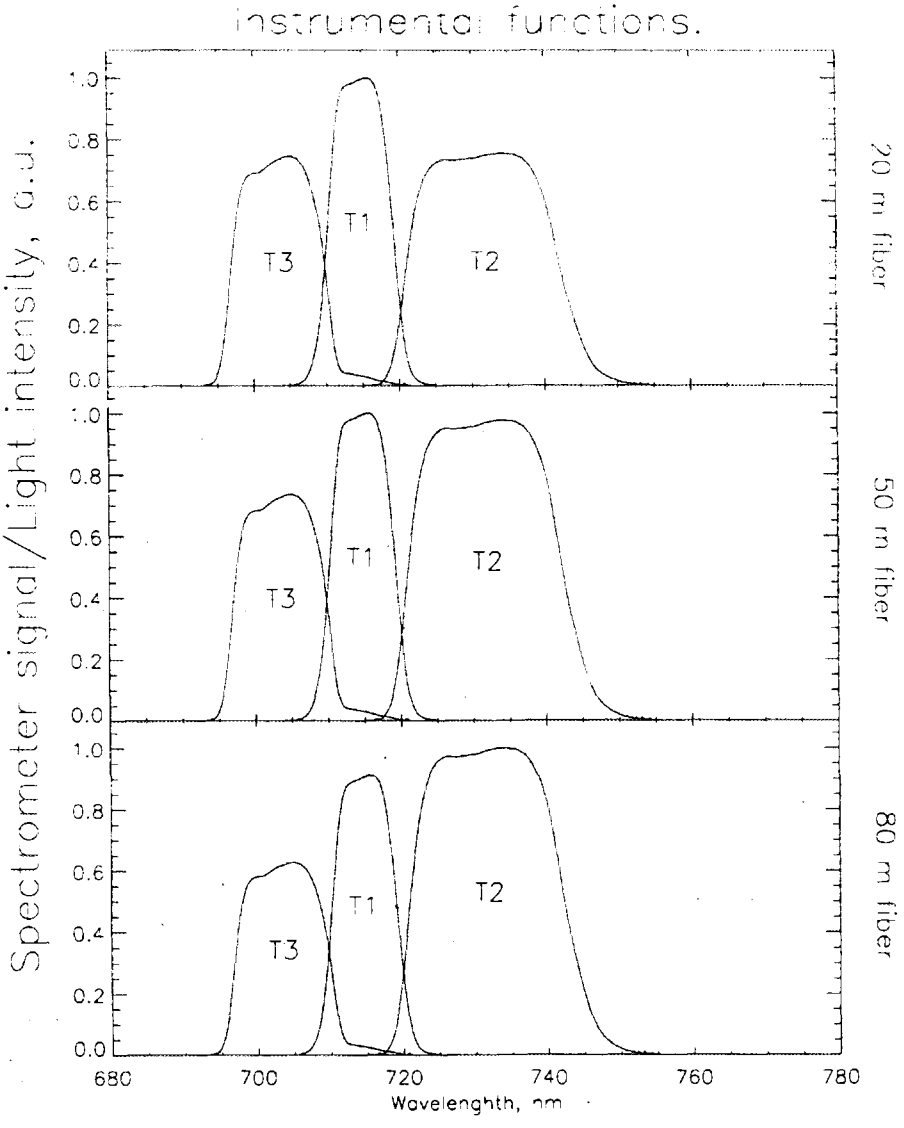

Fig. 7 The instrumental functions for the Thomson scattering system.

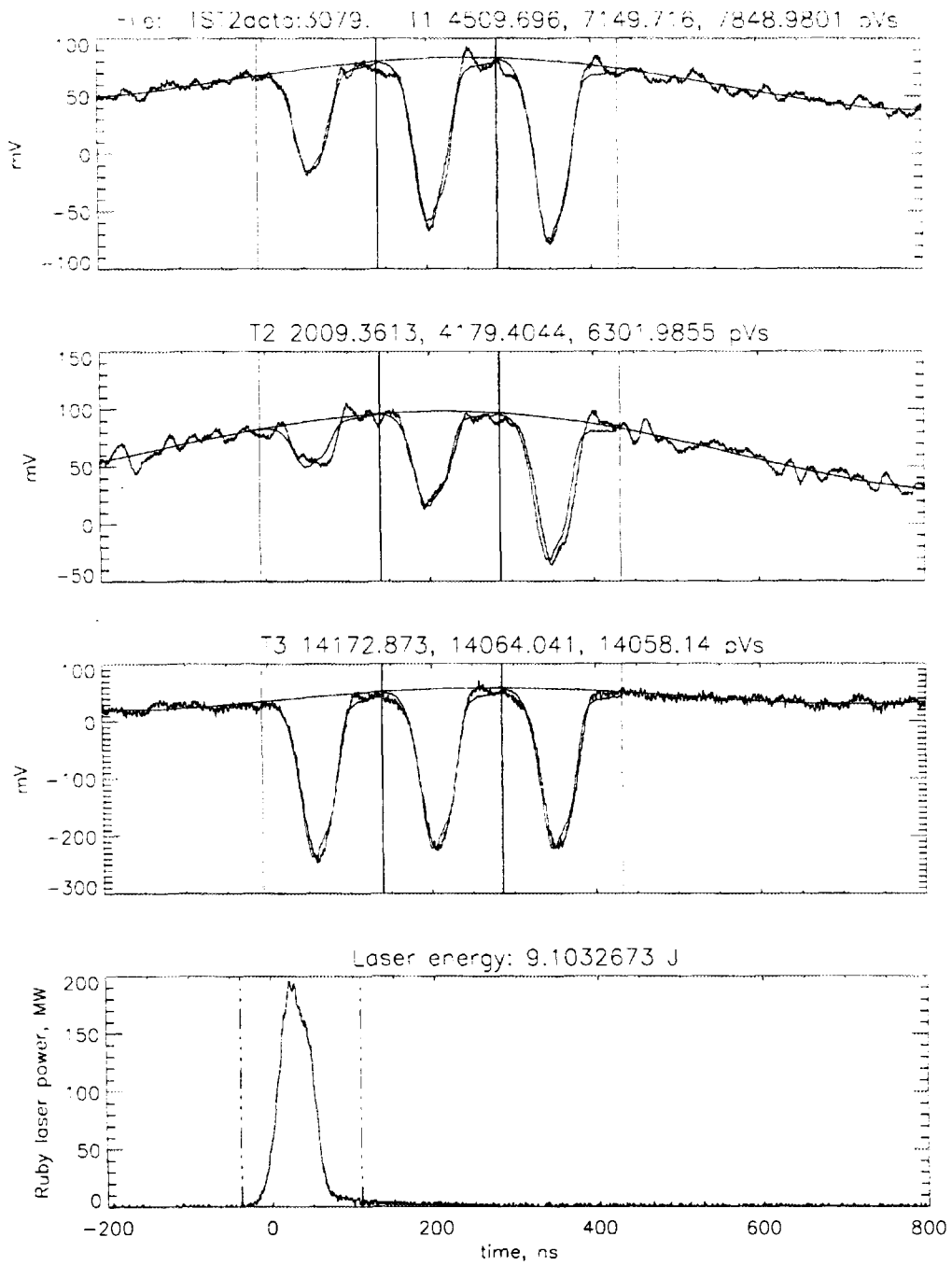

Fig. 8 Example of raw data obtained.

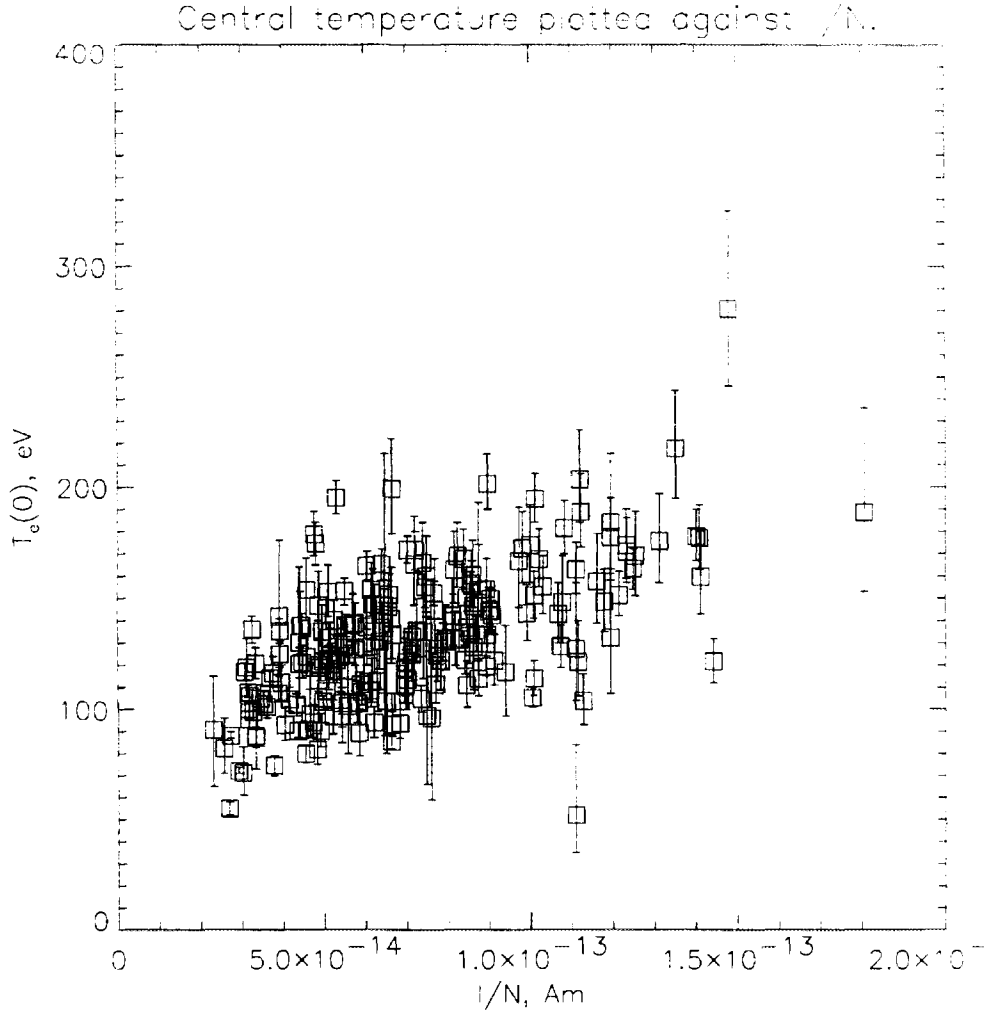

Fig. 9 Temperatures measured in the center of the EXTRAP-T2 plasma.

Thomson scattering in the EXTRAP-T2 reversed-field pinch

A. Welander

Division of Fusion Plasma Physics, Alfvén Laboratory,
Royal Institute of Technology, S-100 44 STOCKHOLM, Sweden

Abstract

A Thomson scattering system has been installed on the EXTRAP-T2 reversed-field pinch (RFP) experiment. The system measures the electron density and temperature in three radial points using three spectral channels. A description of the system, the calibration techniques and examples of data obtained are given. The error bars for the electron temperature measurements are estimated to be $\leq 10\%$ for typical T2-plasmas.

21 pages incl. figures

Key words: Thomson scattering, Reversed-field pinch, Raman scattering

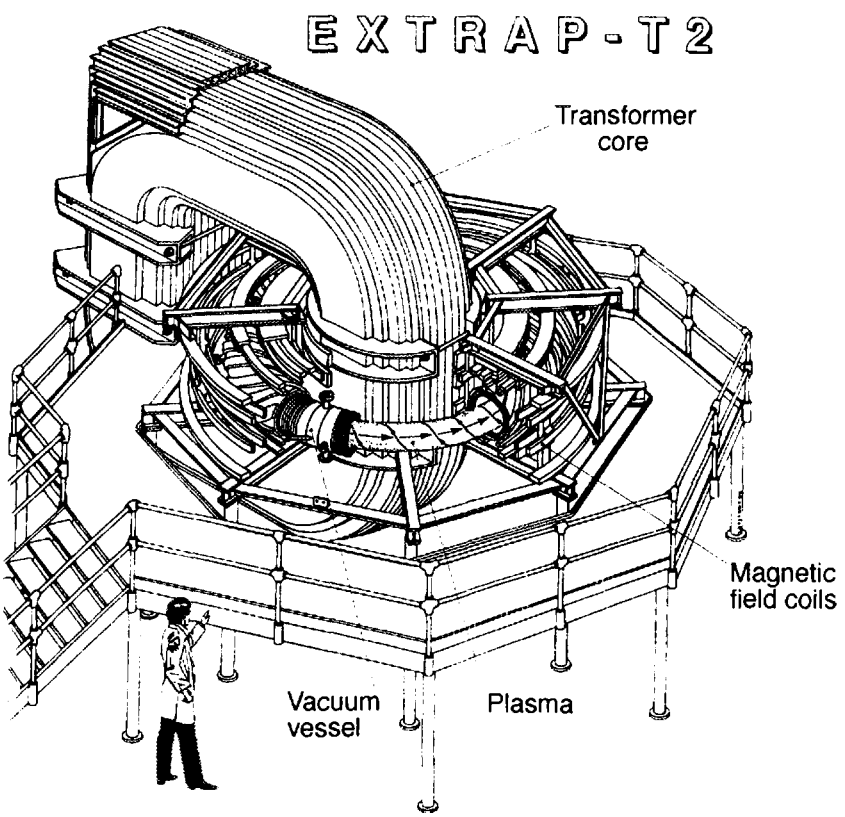

Fig. 1 The EXTRAP-T2 experiment.

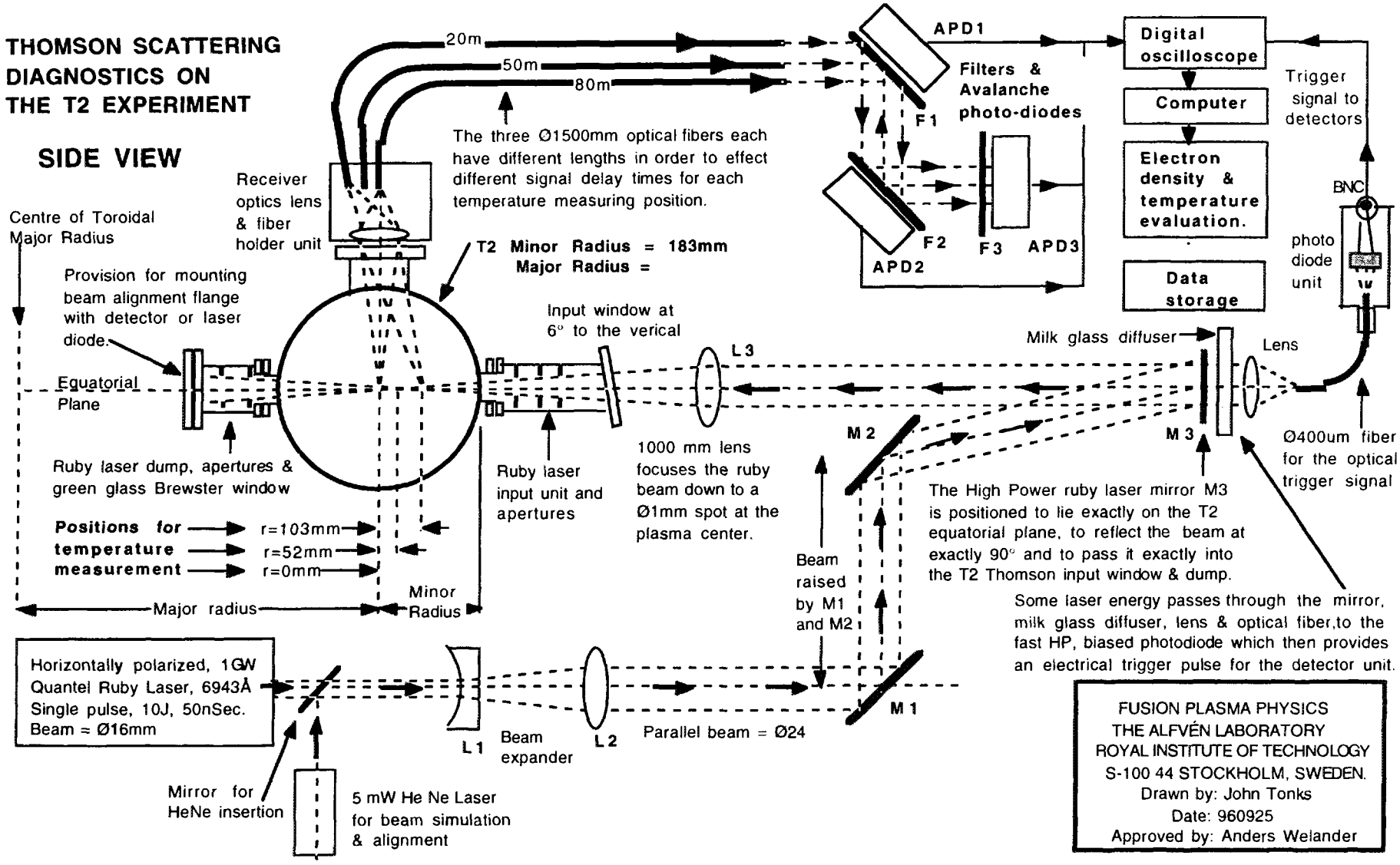

Fig. 2 A schematic view of the Thomson scattering system in use on the EXTRAP-T2 experiment.

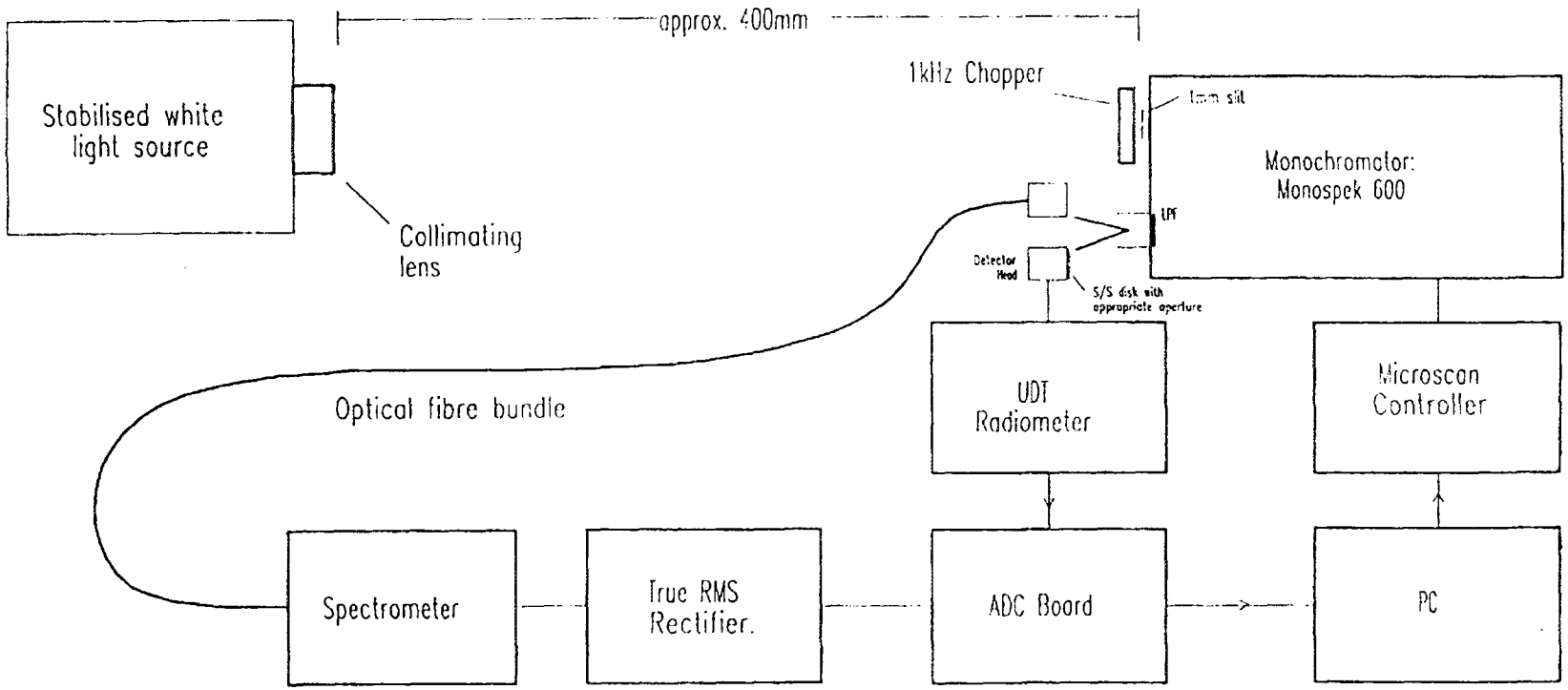

Fig. 3 The arrangement for calibration of the spectrometer.

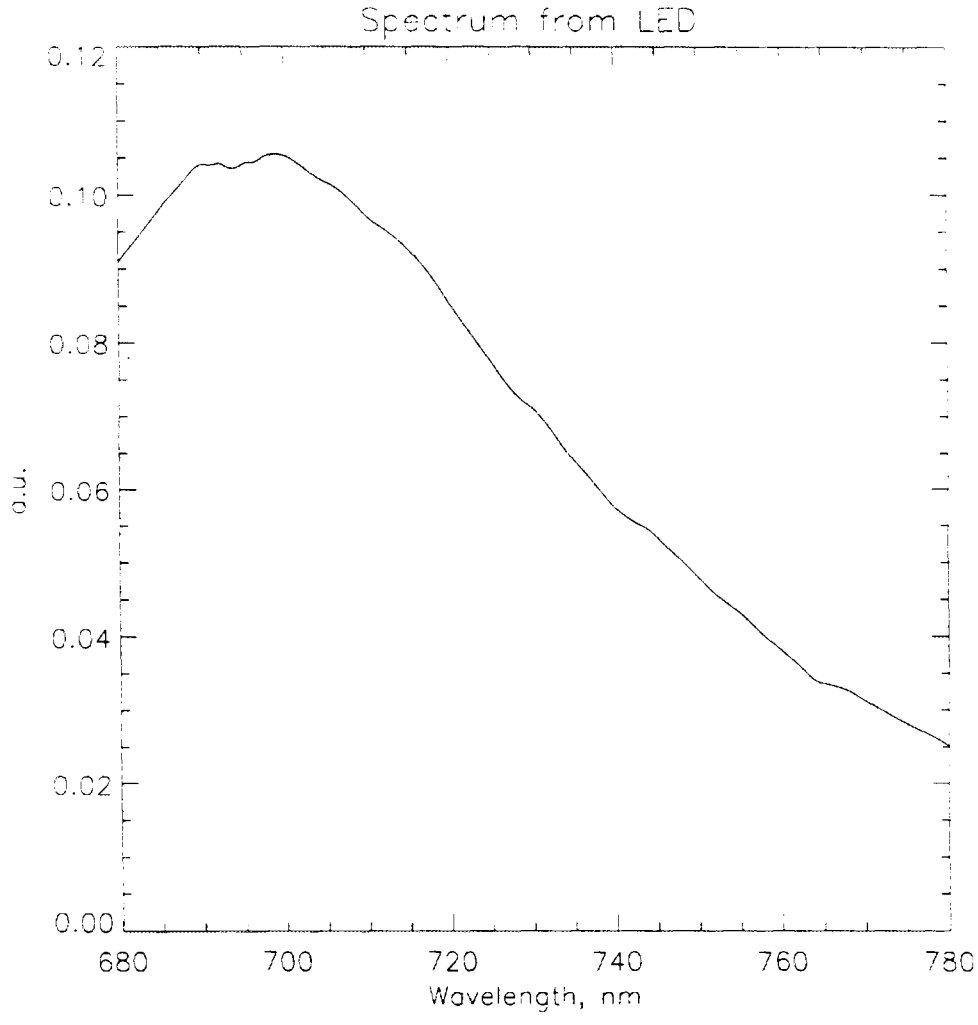

Fig. 4 The spectrum from the light emitting diode which is used in the calibration.

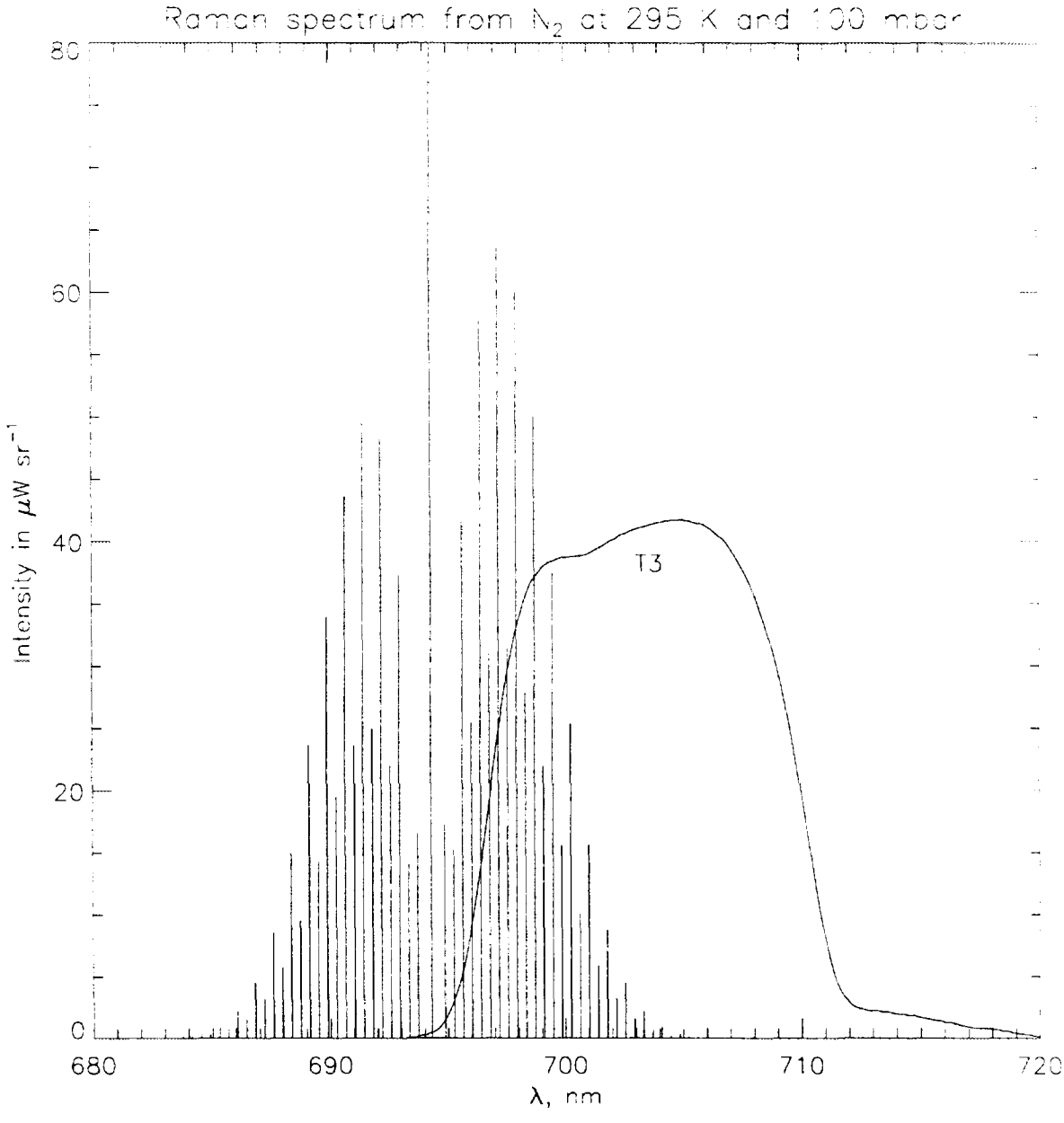

Fig. 5 The Raman spectrum from nitrogen at room temperature is shown together with the instrumental function for spectral channel number 3. The intensity at the ruby laser wavelength, 694.3 nm, is much higher than the Raman lines.

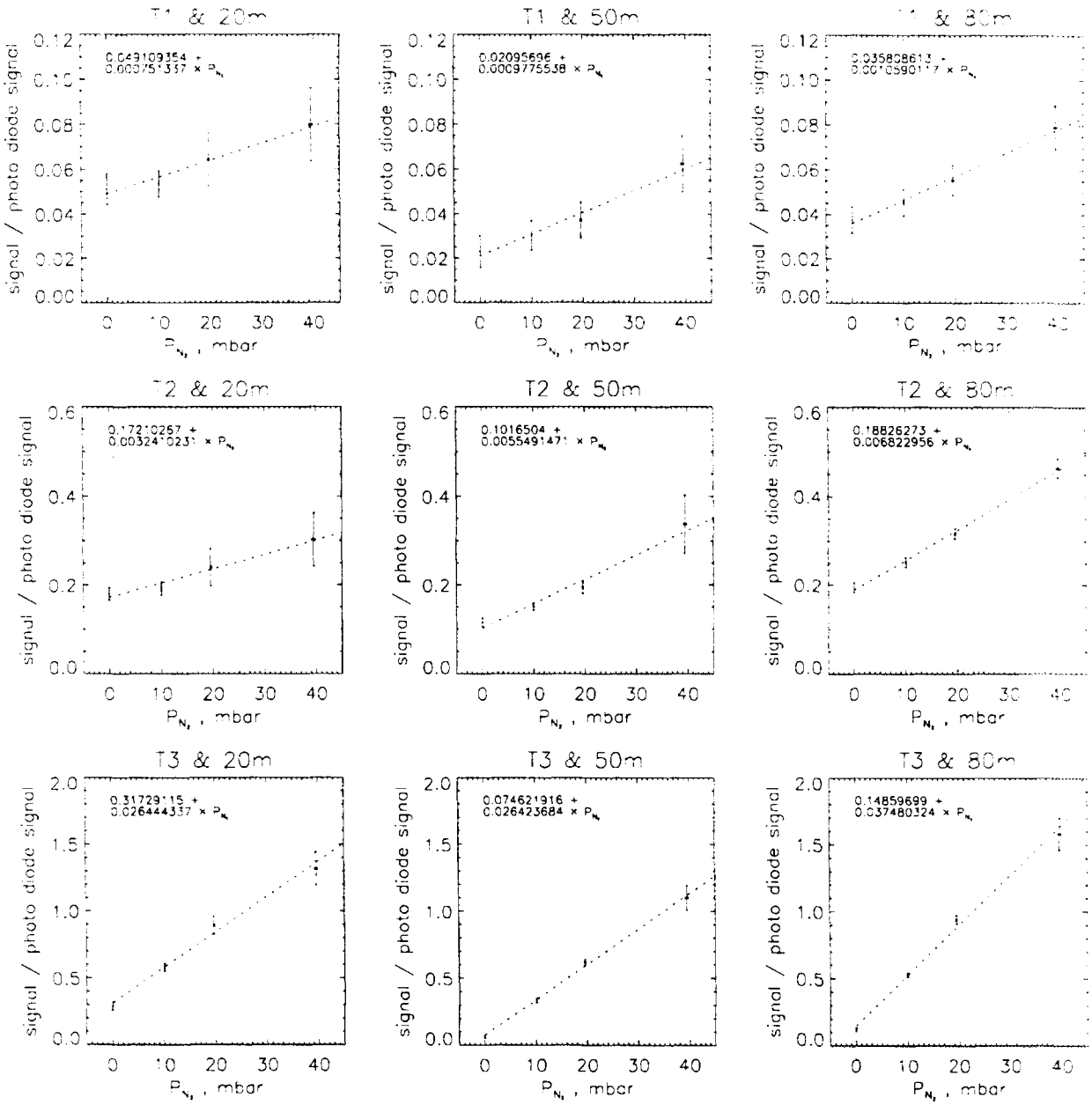

Fig. 6 The signals obtained at different nitrogen pressures.

Raman scattered light is detected by spectral channel number 3 (in the third row).

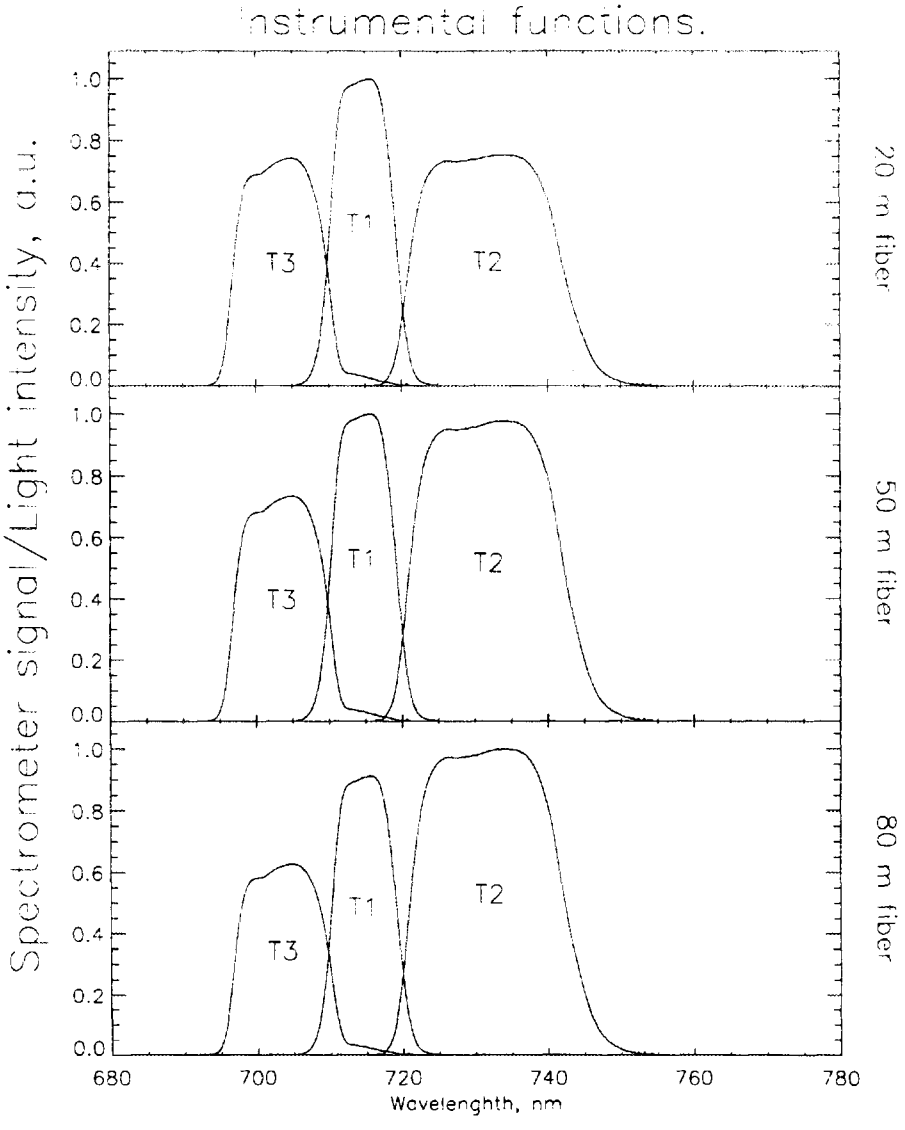

Fig. 7 The instrumental functions for the Thomson scattering system.

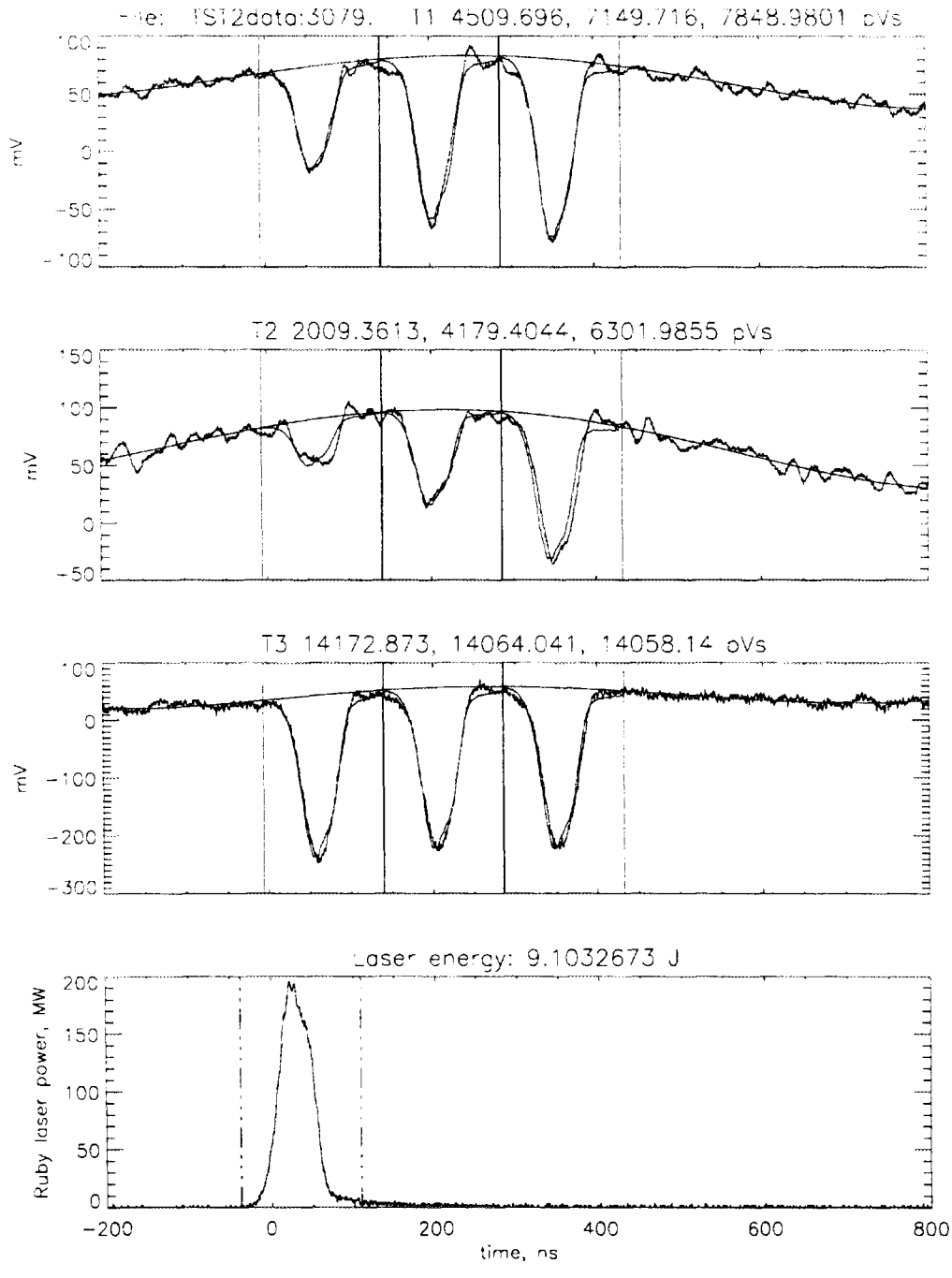

Fig. 8 Example of raw data obtained.

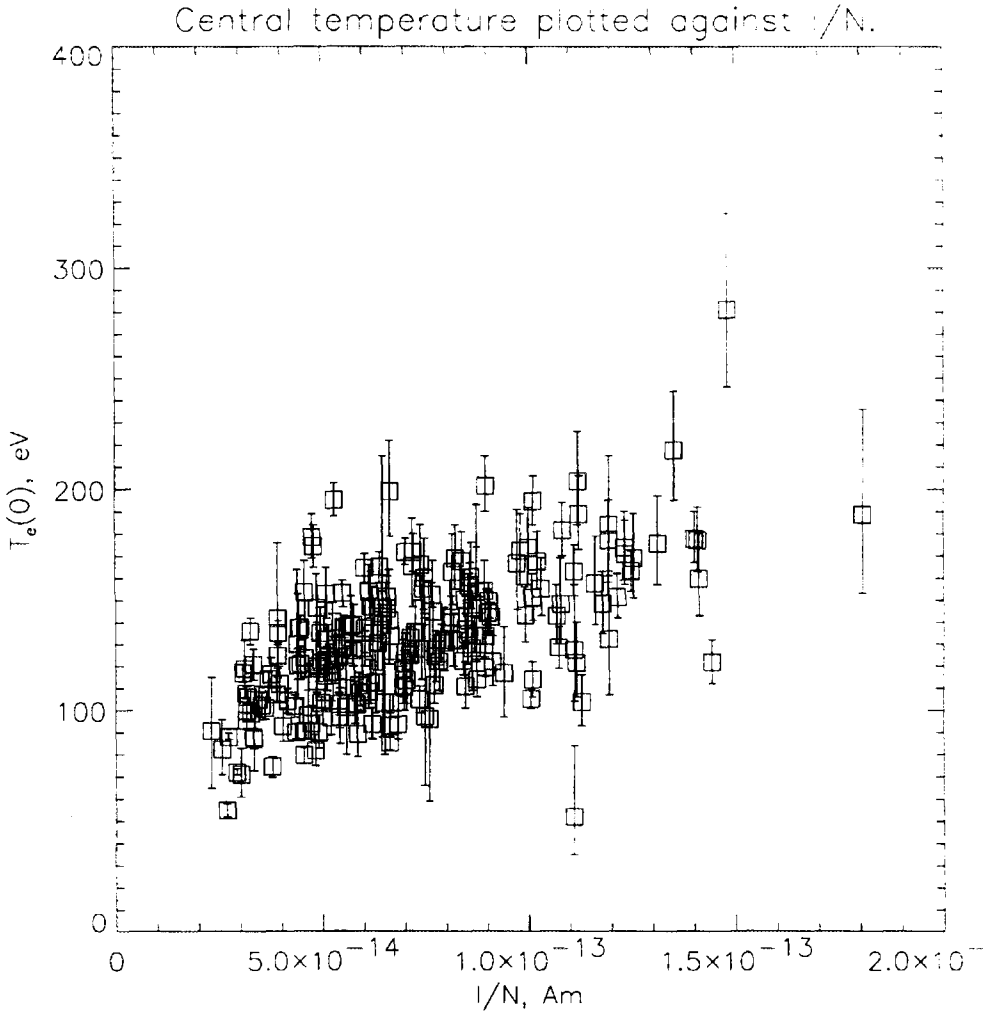

Fig. 9 Temperatures measured in the center of the EXTRAP-T2 plasma.

IRIA-ALF-1996-05
ISRN KTH/ALF/R--96/5--SE

Thomson scattering in the EXTRAP-T2 reversed-field pinch

A. Welander

Division of Fusion Plasma Physics, Alfvén Laboratory,
Royal Institute of Technology, S-100 44 STOCKHOLM, Sweden

Abstract

A Thomson scattering system has been installed on the EXTRAP-T2 reversed-field pinch (RFP) experiment. The system measures the electron density and temperature in three radial points using three spectral channels. A description of the system, the calibration techniques and examples of data obtained are given. The error bars for the electron temperature measurements are estimated to be $\leq 10\%$ for typical T2-plasmas.

20 pages incl. figures

Key words: Thomson scattering, Reversed-field pinch, Raman scattering

We regret that some of the pages in this report may not be up to the proper legibility standards, even though the best possible copy was used for scanning